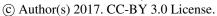Biogeosciences
Discussions

EGU
Open Access

Spatial variations in snowpack chemistry and isotopic composition of NO$_3^-$ along a nitrogen deposition gradient in West Greenland

Chris J. Curtis[1, 5], Jan Kaiser[2], Alina Marca[2], N. John Anderson[3], Gavin Simpson[4, 5], Vivienne Jones[5], Erika Whiteford[3]

5

[1]School of Geography, Archaeology & Environmental Studies, University of the Witwatersrand, Johannesburg, South Africa.
[2]Centre for Ocean and Atmospheric Sciences, School of Environmental Sciences, University of East Anglia, Norwich Research Park, Norwich, UK.
10 [3]Dept of Geography, Loughborough University, UK.
[4]Dept of Biology, University of Regina, Saskatchewan, Canada.
[5]ECRC, Dept of Geography, University College London, Gower Street, London, UK.

Correspondence to: Chris Curtis (christopher.curtis@wits.ac.za)

Abstract. Snowpack chemistry, nitrate stable isotopes and net deposition fluxes for the largest ice-free region in Greenland
15 were investigated to determine whether there are spatial gradients from the ice sheet margin to the coast linked to a gradient in precipitation. Late-season snowpack was sampled in March 2011 at 8 locations within 3 lake catchments in each of 3 regions (ice sheet margin in the east, central area near Kelly Ville and the coastal zone to the west). At the coast, snowpack accumulation averaged 181 mm snow water equivalent (SWE), compared with 36 mm SWE by the ice sheet. Coastal snowpack showed significantly greater concentrations of marine salts (Na$^+$, Cl$^-$, other major cations), ammonium (regional
20 means 1.4-2.7 µmol L^{-1}), total and non-sea salt sulfate (total 1.8-7.7, non-sea salt 1.0-1.8 µmol L^{-1}) than the two inland regions. Nitrate (1.5-2.4 µmol L^{-1}) showed significantly lower concentrations at the coast. Despite lower concentrations, higher precipitation at the coast results in a strong deposition gradient for NO$_3^-$ as well as NH$_4^+$ and non-sea salt sulfate (nss-SO$_4^{2-}$) increasing from the inland regions to the coast (lowest at Kelly Ville 6, 4 and 3; highest at coast 9, 17 and 11 mol ha^{-1} yr^{-1} of NO$_3^-$, NH$_4^+$ and nss-SO$_4^{2-}$ respectively). The $\delta(^{15}N)$ of snowpack NO$_3^-$ shows a significant decrease from the ice sheet
25 margin (-7.5 ‰) to the coast (-11.3 ‰). We attribute the spatial gradient of $\delta(^{15}N)$ in SW Greenland to post-deposition processing rather than differing sources because of 1) the climatic gradient from ice sheet margin to coast, 2) within-catchment isotopic differences between terrestrial snowpack and lake-ice snowpack, and 3) similarities between fresh snow (rather than accumulated snowpack) at Kelly Ville and the coast. Hence the $\delta(^{15}N)$ of coastal snowpack is most representative of snowfall in SW Greenland, but after deposition the effects of photolysis, volatilization and sublimation lead
30 to enrichment of the remaining snowpack with the greatest effect in inland areas of low precipitation and high sublimation losses.

1. Introduction

In recent years it has been demonstrated that anthropogenic nitrogen deposition, primarily from fossil fuel combustion, has reached areas very remote from the original sources, including high latitude sites in the Arctic. Evidence includes contemporary deposition monitoring (AMAP, 2006), the snowpack record of the Greenland ice sheet (Hastings et al., 2009) and palaeolimnological records in Arctic lakes (Holtgrieve et al., 2011). However, contemporary deposition data are sparse in such remote areas due to logistical and cost limitations. According to AMAP (2006), "more observations for NO_3^- in air and precipitation are required to better understand the development of NO_3^- pollution in the Arctic" and Greenland is a striking example of the paucity of data. In addition, stable isotopes of NO_3^- have been used to understand both temporal changes and spatial patterns in N deposition as well as links to ecological changes recorded in Arctic lake sediments. Stable isotope data are even more restricted in the Arctic despite their value for understanding pollutant pathways and ecological impacts, with most published data derived from studies in the centre of the Greenland ice sheet (Hastings et al., 2009; Fibiger et al., 2016) or from Svalbard (Heaton et al., 2004; Tye and Heaton, 2007; Björkman et al., 2014).

The largest ice-free region of Greenland is found in the south-west, where a great number of lakes have been the subject of several limnological and palaeolimnological studies. The region between the edge of the ice sheet, the key international airport hub at Kangerlussuaq and the coastal town of Sisimiut, was selected for an integrated study into the potential effects of nitrogen deposition on Arctic lakes (Figure 1) without the confounding effects of climate change, since there was no significant warming trend in the region for most of the 20th Century (Hanna et al., 2012).This study presents a first attempt to characterise the chemistry and isotopic composition of NO_3^- inputs across an assumed deposition gradient from the ice sheet margin to the coast.

Around half of precipitation in West Greenland falls as snow, with year-to-year variability (e.g. 45 % at Sisimiut and 52 % at Kangerlussuaq from 1994-1997; Yang et al., 1999, and 37-42% at the ice sheet in 2011-12; Bosson et al., 2013). Hence snowpack chemistry (if unchanged following deposition) can provide the data required for estimating annual deposition of pollutants in remote Arctic regions where regular deposition monitoring is not possible due to logistical and financial constraints. In high snowfall regions with a fairly continuously accumulating snowpack, late season snowpack may provide a good estimate of total deposition inputs over the snow season, which may cover more than 6 months in high altitude or high latitude sites (e.g. Rockies – Turk et al., 2001; Ingersoll et al., 2008; Williams et al., 2009). However, in West Greenland the inland areas experience very low precipitation inputs, while sublimation of accumulated snowpack is also important (Bosson et al., 2013). Annual mean precipitation at Sisimiut from 2001-2012 was 631 mm while at Kangerlussuaq it was 258 mm (Mernild et al., 2015). Much greater accumulation of snowpack occurs in the coastal areas, so it is expected that there is a gradient of precipitation, snowpack accumulation and resultant deposition of pollutants from the interior ice sheet margin to the coast.

Here we describe the spatial variation in total inorganic nitrogen (TIN: $NO_3^- + NH_4^+$) and sulfur deposition in snowpack and the isotopic signature of snowpack NO_3^- ($\delta(^{15}N)$, $\delta(^{18}O)$ and $\Delta(^{17}O)$) for three regions in West Greenland. We use the strong climatic gradient to test the hypothesis that both the delivery of TIN deposition and isotopic composition of NO_3^- will differ from the ice sheet margin to the coastal region.

5

2. Methods

2.1 Site selection

As part of a wider study of the ecology and palaeolimnology of low Arctic lakes, deposition study sites were based in three clusters of lake catchments along an assumed deposition gradient from the ice sheet margin to the coast (Figure 1, Table 1), hereafter referred to as ice sheet, Kelly Ville and coastal sites. Three lake catchments were chosen within each region on the basis of previous studies and suitability for (palaeo-)limnological studies reported elsewhere. Five replicated late season snowpack samples were collected within the terrestrial part of each catchment, with a further three replicates obtained from the snowpack on the frozen lake surface. Hence for the purposes of the present study considering spatial gradients, eight samples each from three lake catchments are considered to represent 24 replicated samples within each region. All catchments are located within a narrow latitudinal band around 67° N with a maximum difference in latitude of only 0.2° (22 km). The maximum distance between sites is 153 km (152 km in east-west direction). The distances between regions are much greater than the distance between lake catchments within each region. The central Kelly Ville sites are at least 98 km from the closest coastal site and 33 km from the closest ice sheet site. Within each region, the largest distance between sites is 12 km at the coast, 8 km at Kelly Ville and 5 km at the ice sheet.

20

2.2 Snowpack estimation and sampling

Snowpack depth and density were measured during repeat traverses of each catchment along a grid-based pattern to obtain a spatial coverage of 50-150 measurements per catchment. Depth was measured every 100 m with a graduated pole while density was estimated by taking a snow core of known volume using a 37 mm internal diameter plastic pipe at every 5th measurement point and weighing in the field using a spring balance. Snowpack sampling locations were selected to obtain representative spatial coverage within each lake catchment, recognising the spatial variations in aspect, altitude and snowpack depth where snowpack coverage was unevenly distributed within catchments. Within each catchment, samples were obtained from upper, mid-level and lakeside elevations and different aspects, but logistical constraints limited sampling to just five locations. In addition, three lake snowpack samples on top of the lake ice were obtained from equally spaced

locations along the longest axis of the frozen lake. Hence eight samples per catchment were collected, but comparisons of terrestrial snowpack and snow accumulated on lake ice were also possible.

Snowpack was sampled according to USGS ultra-clean protocols (Clow et al., 2002; Ingersoll et al., 2008, 2009). In
5 summary, all sampling equipment and sample bags were triple rinsed with distilled deionised water (DDIW), with field blanks obtained by rinsing off the sampling shovel and scoop into a clean sample bag with a DDIW wash bottle in the field. Depth-integrated snow samples were collected with a polycarbonate scoop and kept frozen in clean polyethylene bags until processed in the laboratory. Fresh latex gloves for each sample were worn at all times while sampling and processing in the laboratory. Back in the laboratory, snow samples were allowed to thaw at room temperature overnight and then filtered
10 through 0.45 μm nylon membrane filters (Millipore) prior to storage and freezing in 125 ml ultra-clean LDPE bottles. Samples were kept frozen and transported back to the isotope laboratory at UEA where they were stored frozen prior to analysis.

Sampling was carried out in the late winter period to capture as much of the accumulated snowpack as possible without the
15 risk of substantial snowmelt occurring (cf. de Caritat et al., 2005); all total snowpack samples were collected between 22nd March and 1st April 2011. Snowpack profile temperature and physical description were noted as per Ingersoll et al. (2009) for assessment of snowpack status and whether melt was in progress. In addition, to assist with bulk deposition estimates, ad hoc sampling of rainfall and fresh falling snow was carried out on numerous occasions during field campaigns in each region during 2011 and 2012.

20

2.3 Chemical and isotopic analysis

The nitrogen (^{15}N/^{14}N) and oxygen (^{18}O/^{16}O, ^{17}O/^{16}O) isotope ratios of NO_3^- were determined using the denitrifier method (Casciotti et al., 2002; Kaiser et al., 2007). The isotope ratios are expressed as relative isotope ratio differences (isotope deltas) with respect to the international reference materials Air-N_2 for nitrogen isotopes and Vienna Standard Mean Ocean
25 Water (VSMOW) for oxygen isotopes, e.g.

$$\delta(^{15}N/^{14}N, NO_3^-) = \frac{R_{sample}(^{15}N/^{14}N, NO_3^-)}{R_{reference}(^{15}N/^{14}N, NO_3^-)} - 1 \quad (1)$$

Instead of the complete quantity symbols (i.e. $\delta(^{15}N/^{14}N, NO_3^-)$ etc.) we use the short-hand notation $\delta(^{15}N)$, $\delta(^{17}O)$ and $\delta(^{18}O)$. Since $\delta(^{17}O)$ and $\delta(^{18}O)$ are highly correlated, we use the ^{17}O excess, $\Delta(^{17}O)$, instead of $\delta(^{17}O)$ and define it (following Kaiser et al., 2007) as:

30 $$\Delta(^{17}O) = \frac{1 + \delta(^{17}O)}{[1 + \delta(^{18}O)]^{0.5279}} - 1 \quad (2)$$

Biogeosciences
Discussions

Open Access

EGU

The international reference material IAEA-NO-3 was used for calibration of the delta values, using $\delta(^{15}N) = 4.7$ ‰ (vs. Air-N_2), $\delta(^{18}O) = 25.61$ ‰ (vs. VSMOW) and $\delta(^{17}O) = 13.18$ ‰ (vs. VSMOW) (Kaiser et al. 2007), giving $\Delta(^{17}O) = -0.25$ ‰. In addition, the reference materials USGS 34 ($\delta(^{18}O) = -27.93$ ‰, $\Delta(^{17}O) = 0.04$ ‰) and USGS 35 ($\delta(^{18}O) = 57.50$ ‰, $\Delta(^{17}O) = 20.88$ ‰) were used to correct the measurements for oxygen isotope scale contraction. The analytical precision

5 (repeatability) based on repeat sample analysis was 0.2 ‰ for $\delta(^{15}N)$, 0.5 ‰ for $\delta(^{18}O)$ and 0.3 ‰ for $\Delta(^{17}O)$ (10 nmol NO_3^-).

2.3.1 Base cations, SO_4^{2-}, Cl^-

Chloride (Cl^-) and sulfate (SO_4^{2-}) concentrations were measured using ion chromatography on a Dionex ICS-2000 system (Thermo Fisher Scientific) comprising a Dionex Ion Pac AG18 guard column (50 mm x 2 mm), a Dionex Ion Pac AS18

10 analytical column (250 mm x 2 mm), isocratic elution with potassium hydroxide (KOH) at 24 mm, flow rate: 0.250 ml/min, column temperature: 30 °C, with supressed conductivity detection. Standards and ultrapure water blanks (18 MΩ cm, Purelab Ultra) were analysed at the beginning, in the middle and at the end of each sample batch for the calibration of the instrument and to account for any instrument drift during the run. The data were processed using Chromeleon software 6.8 (Thermo Fisher Scientific). The relative analytical precision (repeatability) based on repeat sample analysis was 2 % for both

15 Cl^- and SO_4^{2-}. Major cations, Na^+, K^+, Mg^{2+} and Ca^{2+} were determined using inductively coupled optical emission spectroscopy (ICP-OES; Varian Vista-Pro). Mean instrumental detection limits were 0.1, 0.01, 0.01 and 0.1 μM, respectively, with a relative instrumental precision of 10 %.

2.3.2 Nutrients (NO_2^-, NO_3^-, NH_4^+, phosphate): autoanalyser

20 Nitrite (NO_2^-), NO_3^- (after cadmium reduction to NO_2^-), NH_4^+ and phosphate (PO_4^{3-}, HPO_4^{2-}, $H_2PO_4^-$) concentrations were determined colorimetrically using a Skalar San^{++} autoanalyser. Detection limits of 0.1 μM (for NO_3^- and NH_4^+) and 0.01 μM (for NO_2^- and phosphate) were achieved, with a relative instrumental precision of 4 %.

2.4 Statistical analysis

25 For all snowpack chemistry and isotope data, statistical analysis was first performed on aggregated regional data (15 catchment replicates plus 9 lake snow replicates; n=24 per region). Subsequent analyses were performed to compare catchment snowpack between regions, lake ice snowpack between regions, and catchment versus lake ice snowpack within regions. Generalized linear mixed models (GLMM) were used to investigate how snowpack chemistry and isotope variables varied between regions. A random intercept was included in the model to account for clustering in the data at the catchment

30 level. Snowpack chemistry variables were modelled using a Gamma GLMM with log link function to account for non-constant variance. Stable isotope variables were modelled using a Gaussian GLMM with identity link function. Additional

models explored differences in snowpack chemistry and stable isotopes between samples of catchment snow and snow over lake ice by including sample type, region, and their interaction terms in the fitted models.

Post-hoc pairwise comparison of the GLMM-estimated regional means was performed using Tukey contrasts and the generalized linear hypothesis testing (GLHT) framework. For models of differences in snow sample type (terrestrial versus lake ice) post-hoc comparisons were restricted to comparison of sample type within region using appropriate contrast matrices.

All statistical analyses were performed using the R statistical language (version 3.3.2; R Core Team, 2016) with the lme4 package (version 1.1.12; Bates et al, 2015) for fitting GLMMs and the multcomp package (version 2.4.6, Hothorn et al, 2008) for GLHT post-hoc comparisons.

3. Results

3.1 Catchment scale snowpack depth and SWE estimation

Estimates of snowpack depth and snow water equivalents (SWE) are presented in Table 2. Note that snow water equivalent calculations were carried out for the subset of points at which snow mass was measured in the snow tube and then corrected for mean snow depth across each catchment based on the much larger number of snow depth measurements. Snow density ranged from 0.20 to 0.34 g cm^{-3}, remarkably similar to the datasets used in the wide-ranging snow depth-SWE study of Sturm et al. (2010) (0.21-0.34 g cm^{-3}).

Snow depth measurements confirm that there is a major difference in snowpack accumulation from 16 to 20 cm mean catchment snow depth (max. 103 cm; overall 35.7 mm SWE) close to the ice sheet, up to 50-74 cm mean catchment snow depth (max. 260 cm; overall 180.8 mm SWE) at the coast. Depth and SWE are slightly higher at the central Kelly Ville catchments relative to the ice sheet sites, but all are still much lower than the coastal sites. At the two inland regions, snow cover is much more patchy than at the coast, where continuous cover was found except on the steepest slopes (Figure 2).

3.2 Snowpack sampling and chemistry

Details of snowpack samples for chemical and isotopic analysis are provided in Table 3a (terrestrial) and 3b (lake ice snowpack). At the ice sheet, *sampled* terrestrial snowpack varied from 24 to 103 cm depth while *sampled* lake ice snowpack reached only 23 cm maximum depth, reflecting the heterogeneous snow distribution around the catchment and suggesting

wind redistribution of the snow. Sampled terrestrial snowpack depth had a smaller range at the Kelly Ville catchments, from 23 to 65 cm, and again the lake ice snow depth was much smaller, reaching only 30 cm maximum depth. At the coastal sites, terrestrial snowpack depths from 28 to 240 cm were sampled while lake ice snow ranged from 19 to 60 cm depth. During the sampling period, air temperatures were all well below 0 °C at the ice sheet and Kelly Ville sites, reaching a maximum of -6

5   °C. However, during sampling of the coastal snowpack, air temperatures were slightly above freezing, suggesting that some snowmelt may have been occurring during the sampling period (Table 3a-b). Snowpack temperatures were only just below zero at the coastal sites and melting was observed in the lake ice snowpack at site AT1.

3.3 Regional comparison of aggregated snowpack data

10   Concentrations of major ions in west Greenland snowpack are very low (<5 μmol L^{-1}) except for Mg^{2+}, SO_4^{2-} and the sea-salt associated ions Na^+ and Cl^- (Table 4). Analysis of the aggregated snowpack data shows that there are significant differences for most measured analytes except NO_2^- between the coastal sites and both the Kelly Ville and ice sheet margin sites, while snowpack composition is very similar between the two inland regions (Table 4). For NH_4^+, SO_4^{2-}, Cl^- and all base cations, concentrations are significantly higher in coastal snowpack than in the Kelly Ville or ice sheet regions (except for no

15   significant differences between the coast and ice sheet sites for NH_4^+ and Ca^{2+}). The sea-salt-associated ions Na^+ and Cl^- are highly correlated ($r=0.999$, $p<0.01$) and concentrations are an order of magnitude greater at the coast than inland. Mg^{2+}, K^+ and SO_4^{2-} are also very highly correlated with Cl^- ($r>0.95$, $p<0.01$). The nutrients NO_3^- and PO_4^{3-} show an opposing pattern to the sea salt related ions, with significantly lower concentrations in coastal snowpack than at inland sites and weak, negative correlations with Cl^- (NO_3^-: $r=-0.392$, $p<0.01$; PO_4^{3-}: $r=-0.277$, $p<0.05$).

20

In order to investigate the influence of non-sea salt atmospheric sources of ions, the proportion of sea salt contributions was subtracted using Cl^- as a tracer of sea salt inputs and the relatively constant ionic proportions of major ions in seawater (Henriksen & Posch, 2001). For non-sea salt sulfate, the pattern of snowpack concentrations is similar to total measured values, with the highest mean concentrations at the coast which are significantly greater than inland, although mean non-sea

25   salt concentrations are all very low (1.0-1.8 μmol L^{-1}). Non-sea salt Mg^{2+} is significantly lower at Kelly Ville than elsewhere, while non-sea salt Ca^{2+} increases significantly from the coast towards the ice sheet, presumably due to wind-blown minerogenic sources. There are no significant differences for non-sea salt K^+ and negative values for non-sea salt Na^+ suggest either non-sea salt sources of Cl^- or snowpack losses of Na^+, perhaps through preferential elution pathways.

For nutrients, concentrations in seawater are assumed to be negligible hence snowpack concentrations are assumed to be due

30   entirely to non-sea salt atmospheric inputs. Nitrate concentrations are very low at all sites but significantly lower ($p<0.0001$) at the coast (mean 1.5 μmol L^{-1}) than at Kelly Ville (mean 2.3 μmol L^{-1}) or the ice sheet (mean 2.4 μmol L^{-1}), with no significant difference between the inland regions. Mean NH_4^+ concentrations are also low, but significantly higher in coastal snowpack (2.7 μmol L^{-1}) than Kelly Ville (1.4 μmol L^{-1}). Nitrite levels were negligible in all regions.

3.4 Catchment snowpack versus lake ice snowpack

Exploratory data analysis of separate terrestrial snowpack (n=5 per catchment) and lake ice snowpack (n=3 per catchment) was carried out to determine whether there were within-catchment differences in snowpack chemistry between catchment

5 slopes (with very heterogeneous snow cover) and the relatively homogenous snow cover on the frozen lake. Mean lake ice snowpack concentrations were higher than terrestrial snowpack concentrations for all ions except for a few cases with very low ionic concentrations of <3 µmol L^{-1}, with the difference being most pronounced at the coastal sites (Table SI 1). While very few of these differences were statistically significant except at the coast (P<0.05 for all plotted ions), the pattern of higher lake ice snowpack concentrations was remarkably consistent (Figure 4). For NO_3^-, significantly higher concentrations

10 were found in lake ice snowpack at the coast (p=0.028) and Kelly Ville (p=0.0042) but the difference was not quite significant for the ice sheet sites (p=0.0731) – noting that only 3 replicated lake ice snowpack samples resulted in large standard errors.

The only sites where melting snow was observed during sampling were at the coast, raising the possibility that in coastal

15 catchments, the snowpack on lake ice could be the recipient of meltwater drainage from catchment slopes whereby preferential elution from catchment snowpack could explain the higher concentrations in the lake snow. Alternatively, losses of some ions such as NO_3^- back to the atmosphere may be greater on catchment slopes (see Discussion below considering stable isotope data). Despite differences between catchment snow and lake ice snowpack, the general patterns of higher major ion concentrations at the coast but lower nutrients (as seen in the aggregated catchment data) is repeated.

20

3.5 Stable isotopes

For aggregated snowpack $\delta(^{15}N)$ there are significant differences (p<0.001) between coastal and inland regions (as with major ion chemistry) with the lowest mean values at the coast (-11.3 ‰) and the highest at Kelly Ville (-5.7 ‰) (Table 4). There are no significant differences in $\delta(^{18}O)$ with mean values of 81.7-83.3 ‰, across all regions. None of the measured

25 isotopes show significant differences between inland regions. Values of $\Delta(^{17}O)$ in catchment snowpack range from 30.8 ‰ at the coast to 34.4 ‰ at Kelly Ville, again with significantly lower values in coastal snowpack than for inland regions (p<0.01).

3.6 Deposition estimates

In addition to the analysis of accumulated snowpack in the study regions, ad-hoc sampling of fresh snow and rainfall was carried out on numerous occasions during late winter, summer and autumn field campaigns. Unfortunately, most of the bulk deposition samples collected were subject to major contamination by bird strikes by the northern wheatear (*Oenanthe*
5   *oenanthe*) which finds any prominent vertical structures in the low Arctic scrub an irresistible vantage point, despite attempts to fit various configurations of bird deterrent devices. However, a small number of uncontaminated rainfall samples were collected along with fresh snowpack samples where a surface accumulation of falling snow was collected within a few hours of being deposited (Table 5).

10 Fresh snow collected from coastal sites in 2011 had slightly higher nutrient concentrations compared to catchment snowpack but had very low concentrations of sea salt related ions, indicating that in the fresh falling snow the influence of seasalt inputs was minimal. Presumably marine aerosols accumulate in the snowpack over winter, which may explain the higher concentrations of NH_4^+ as well as SO_4^{2-} at the coast. Fresh snow collected at Kelly Ville in April 2011 also had slightly higher concentrations of NO_3^- and NH_4^+ than regional snowpack but had very similar major ion concentrations. Four rainfall
15 samples from the Kelly Ville region in 2011 had variable concentrations of NO_3^- (1.3- 7.8 µmol L^{-1}) but the mean of 4.0 µmol L^{-1} was higher than the regional snowpack (mean 2.3 µmol L^{-1}) while NH_4^+ concentrations in the rainfall were slightly lower than the snowpack (Table 5). Several rainfall samples were also collected from the ice sheet region, again showing c. 50% higher mean NH_4^+ (3.1 µmol L^{-1}) and NO_3^- (3.4 µmol L^{-1}) than the snowpack.

20 Logistical challenges prevented the routine monitoring of non-snowpack precipitation, and while around half of annual precipitation falls as snow in West Greenland, this does mean that annual deposition fluxes can only be estimated using best available data. In this region, we assume that snowpack concentrations of atmospherically derived ions are representative of total annual precipitation and hence can obtain a first approximation of deposition fluxes by using mean snowpack solute concentrations with measured annual precipitation data at Sisimiut and Kangerlussuaq (Mernild et al., 2015) and scaled for
25 ice sheet data at SS903 from 2011-12 (Bosson et al., 2013). Estimated deposition loads based on mean snowpack chemistry and mean 2001-2012 precipitation levels for Sisimiut (coast) and Kangerlussuaq (inland regions) are shown in Table 6.

While NO_3^- concentrations are lower at coastal sites than inland, higher precipitation levels at the coast lead to 18-62 % greater NO_3^- deposition than inland. For NH_4^+ where coastal sites have both higher concentrations and higher precipitation,
30 estimated deposition loads are around 3-5 times higher at the coast than inland. Overall, total N deposition at the coast is therefore estimated to be 1.9-2.8 times higher than for the inland regions. For non-sea salt SO_4^{2-} the deposition at the coast is also 2.7-4.4 times higher than inland.

4. Discussion

4.1 Precipitation chemistry

The gradient in precipitation from the coast to the ice sheet has been attributed by Mernild et al. (2015) to katabatic winds moving downslope from the ice sheet interior, distance from oceanic moisture sources and orographic enhancement by

5   coastal mountains, all contributing to much greater precipitation at the coast relative to areas further inland towards the ice sheet. There is a strong gradient in the chemistry of snowpack from inland to the coast which is primarily driven by the greater influence of marine inputs (sea spray and aerosols) at the coast, clearly shown by highly elevated concentrations of Na^+ and Cl^- (cf. coastal snowpack in Svalbard studied by Tye & Heaton, 2007) but also by separate gradients in atmospheric pollutant deposition. Concentrations of NH_4^+ ($p=0.0017$ for coast-Kelly Ville) and nss-SO_4^{2-} ($p<0.05$) are greater in coastal

10 snowpack than inland, but concentrations of NO_3^- ($p<0.0001$) are lower at the coast. Hence there is clearly an interaction between dilution effects of greater precipitation at the coast and differential pollutant inputs and presumably pathways from inland to coastal regions (see below).

Snowpack solute concentrations in this study are comparable to values recorded in studies on the Greenland ice sheet.

15 Fischer et al. (1998a) studied chemistry of recent firn along ice sheet transects and recorded a range of 110-150 ng g^{-1} (1.8-2.4 µmol L^{-1}) NO_3^- and 70-110 ng g^{-1} (1.5-2.3 µmol L^{-1}) sulfate for central Greenland. Burkhart et al. (2004) recorded a mean NO_3^- of 2.9 µmol L^{-1} in surface snow at Summit from 1997-1998 (range 0.4-34.4 µmol L^{-1}) while a later study indicated recent peaks of 2-5 µmol L^{-1} in 6 ice cores (Burkhart et al., 2006). Dibb et al. (2007) studied daily snowpack chemistry at Summit from 1997-98 and then from August 2000-August 2002, and recorded overall mean concentrations of

20 0.5 µmol L^{-1} for NH_4^+ (monthly mean range 0.1-1.4 µmol L^{-1}) and 3.2 µmol L^{-1} for NO_3^- (monthly mean range 1.3-6.7 µmol L^{-1}). Mean SO_4^{2-} was 0.7 µmol L^{-1} (monthly mean range 0.2-2.3 µmol L^{-1}) while mean Na^+ was 0.4 µmol L^{-1} and Cl^- was 0.8 µmol L^{-1}. In equivalence terms, NO_3^- constituted the dominant ion in fresh snow at Summit while sea salt ion concentrations were negligible, much lower than the terrestrial snowpack in our study and reflecting the much greater distance from the coast of the ice sheet studies. Dibb et al. (2007) found that NO_3^- was the only ion having a higher concentration in fresh snow

25 compared with buried layers, but the difference, presumably due to postdepositional processing, was only 9%. More recent samples at Summit showed mean concentrations of 2.8 and 5.2 µmol L^{-1} for the 2010 and 2011 seasons (Fibiger et al., 2016). Our results are also within the range of other studies of Arctic precipitation and ice cores. Kekonen et al. (2002) recorded peak concentrations of 3-4 µmol L^{-1} for NO_3^- and 4-5 µmol L^{-1} for NH_4^+ during the 1980s in Svalbard ice cores. Tye & Heaton (2007) found concentrations of 1.7-3.1 µmol L^{-1} NO_3^- and 1.2-1.7 µmol L^{-1} for NH_4^+ in Svalbard snowpack. In the

30 AMAP synthesis of Arctic precipitation chemistry data (Hole et al., 2006a), NO_3^- concentrations for the period 1980-2005 ranged from 0-10 µmol L^{-1} but the great majority of annual mean values were <4 µmol L^{-1}. However, the majority of stations showed higher winter than summer precipitation concentrations, unlike our study where analysis of ad hoc rainfall samples suggested higher concentrations of NO_3^- and NH_4^+ in rainfall relative to snowpack (Table 5). Sulfate concentrations were

much more spatially variable, but the great majority of annual mean concentrations were <10 µmol L^{-1} and some regions showed higher summer than winter concentrations (Hole et al., 2006a). De Caritat et al. (2005) carried out a wide-ranging snapshot survey of Arctic snowpack chemistry and found snowpack concentrations at Pittufik (NW Greenland) of 5.7-8.9 µmol L^{-1} for NO$_3^-$ and 9.9-12.8 µmol L^{-1} for SO$_4^{2-}$, with median values across their Arctic survey of 3.5 and 9.9 µmol L^{-1}

5   respectively. Jaffe and Zukowski (1993) recorded 2.6 and 1.9 µmol L^{-1} for NO$_3^-$ and SO$_4^{2-}$ in Alaskan snowpack.

Hence the chemistry of SW Greenland snowpack is comparable to the Greenland ice sheet and other areas of the Arctic remote from pollution sources, but with lower acid anion concentrations than more polluted regions of the Arctic such as parts of the Russian Federation and NW Europe (De Caritat et al., 2005; Hole et al., 2006b). Snowpack concentrations in

10   this part of the Arctic are also generally lower than those recorded in remote alpine systems such as the Rockies (e.g. 10-12 µmol L^{-1} for NO$_3^-$ and 3-6 µmol L^{-1} for NH$_4^+$; Williams et al, 2009). Sources of nitrogen and sulfur compounds in the Arctic include long-range transport of fossil fuel combustion products from e.g. large smelters in the Russian Federation, shipping on Arctic sea routes, volcanic activity (e.g. Iceland, Alaska) and biomass combustion from natural or anthropogenic fires in the boreal forest zone (Hole et al., 2006b). The mix of Eurasian and North American sources for both S and N was found to

15   be consistent across the Greenland ice sheet, based on emission inventories and ice core records (Fischer et al., 1998b), but it may be assumed that local shipping sources would be greatest for the coastal region.

4.2 Deposition estimates

There are very few data for recent atmospheric deposition in Greenland, but there have been studies of snowpack and ice

20   core records of pollutants on the Greenland ice sheet (e.g. Dye2, 200 km from Kangerlussuaq; Dye3, 380 km; Summit, 800 km; Burkhart et al., 2006). Therefore, despite the lack of contemporary deposition data for the region, there are numerous records of relative change in nitrogen deposition loads over the past 200 years or more.

Ice-core records from Greenland show that increases in NO$_3^-$ commenced in the latter half of the nineteenth century

25   (Mayewski et al., 1990; Fischer et al., 1998b; Burkhart et al., 2006). Greenland ice core records closely follow the emissions inventories for Europe and North America over this period (Burkhart et al., 2006). Current NO$_3^-$ concentrations are double the pre-industrial levels across the Greenland ice sheet (Fischer et al., 1998b; Hastings et al., 2009). Burkhart et al. (2006) calculated 1789-1994 deposition fluxes for six ice sheet cores to range from 0.13 to 0.59 kg ha^{-1} a^{-1} with mean N deposition flux derived from snow pits at Summit of 0.5 kg ha^{-1} a^{-1} as NO$_3^-$ (0.11 kgN ha^{-1} a^{-1}; Burkhart et al., 2004). These fluxes are

30   double the pre-industrial values for both wet and dry NO$_3^-$ deposition (Fischer et al., 1998a). Fluxes of NO$_3^-$ derived from ice cores since the 1960s ranged from 0.5 (at D3) to 1 kg ha^{-1} a^{-1} at Gits (NW Greenland) in the study of Burkhart et al. (2006).

Fluxes of NO_3^- deposition in the current study range from 0.08 to 0.13 kg ha^{-1} a^{-1} which are remarkably similar to the fluxes recorded at Summit by Burkhart et al. (2004). Total inorganic N deposition fluxes are 2-3 times higher at the coast (0.37 kg ha^{-1} a^{-1}) than inland, primarily due to NH_4^+, reflecting both the higher precipitation but also possibly local sources, especially of NH_4^+. Unlike NO_3^- there has been no similar increasing trend in NH_4^+ in ice core records over the past 200 years

5   (Savarino & Legrand, 1998). Other studies of industrial sources of contaminants indicated by unsupported ^{210}Pb and weapons ^{137}Cs in lake sediment cores have also found a strong gradient of increasing deposition from the ice sheet to the coast in this region (Bindler et al., 2001a, b). Isotope ratios of Pb indicate that Western Europe is a major emissions source for southern Greenland (Bindler et al., 2001b).

10   Burkhart et al. (2004) reviewed several studies demonstrating that deposition flux (but not concentration) is strongly dependent on snow accumulation (Legrand & Kirchner, 1990), which is consistent with our results showing the much higher deposition flux at the coast where the snowpack is much greater than inland, even if only on a seasonal basis (unlike the ice sheet). Unlike larger-scale studies of Arctic precipitation (Hole et al., 2009), NO_3^- deposition appears to be of a similar magnitude in charge-equivalent terms to nss- SO_4^{2-} deposition in inland regions of West Greenland, while TIN deposition is

15   almost double nss-SO_4^{2-} deposition (Table 5). At the coast, NO_3^- deposition (9 mol ha^{-1} a^{-1}) is much lower than nss-SO_4^{2-} (11 mol ha^{-1} a^{-1}) while NH_4^+ is comparable in charge-equivalent terms (17 mol ha^{-1} a^{-1}), possibly suggesting an influence of ammonium sulfate aerosols (Fisher et al., 2011; Paulot et al., 2015). Local urban, marine or shipping emissions could also account for higher deposition fluxes of all these ions in coastal snowpack, especially given the proximity of the town and port at Sisimiut, but since NO_3^- fluxes are much less enhanced at the coast than either NH_4^+ or nss-SO_4^{2-} a dominant

20   deposition pathway via ammonium sulfate (Fisher et al., 2011) seems most likely. Ammonium and sulfate are highly correlated in coastal snowpack (natural logs of concentrations; r=0.740, t=5.154, df=22, p=3.63e-05) which provides supporting evidence for this pathway.

Modelled wet deposition of nss-SO_4^{2-} for West Greenland in a global analysis was found to be in the region of 0.2 kg ha^{-1} a^{-1}

25   S (Vet et al., 2014), which falls in the middle of the spatial range suggested by our study (0.08 – 0.35 kg ha^{-1} a^{-1}). The same modelling study indicated wet deposition of total N to be <1 kg ha^{-1} a^{-1}, which includes the range of estimates in our study. Nitrogen deposition levels in West Greenland snowpack (assuming 50% of deposition as snow) are comparable to those found in Svalbard snowpack, estimated at 0.059 kg ha^{-1} a^{-1} for NO_3^--N and 0.03 kg ha^{-1} a^{-1} for NH_4^+-N in 2001 (Tye and Heaton, 2007) and NO_3^--N deposition rates (wintertime, snow-derived only) to Alaskan snowpack of 0.07-0.12 kg ha^{-1} a^{-1}

30   (Jaffe & Zukowski, 1993). These values are much lower than those found in high altitude snowpack in the Rockies of the USA, for example 1.43-1.71 and 0.46-0.81 kg ha^{-1} a^{-1} for NO_3^--N and NH_4^+-N in the study of Williams et al (2009). Likewise, higher deposition loads are recorded in the Russian Arctic, where total N and S deposition loads range from 0.75-3.10 and 0.40-3.00 (much higher close to smelters) kg ha^{-1} a^{-1} (Hole et al., 2006a).

4.3 Stable isotopes

Isotope delta values of snowpack NO_3^- in the current study are comparable to the few other published studies in the Arctic from seasonal snowpack (as opposed to accumulating snow on the ice sheet). Heaton et al. (2004) sampling snowpack in Svalbard during 2001-2003 recorded δ (^{15}N) in the range -4 to -18 ‰ while $\delta(^{18}O)$ values fell in the range 42-76 ‰ (60-85

5 ‰ when accounting for organic contamination) while Tye and Heaton (2007), also in Svalbard, found seasonal snowpack δ (^{15}N) fell in the range -7 to -18 ‰ while $\delta(^{18}O)$ values fell in the range 74-78 ‰. The snowpack data presented here are slightly higher but largely overlapping with the Svalbard studies, with the mean δ (^{15}N) of -11 ‰ for coastal catchments being lower than most of the non-polar studies reviewed by Heaton et al. (2004).

10 There are few published studies on the triple isotope analysis of O in NO_3^- globally. Although $\delta(^{18}O)$ values in our study are in a similar range (81-84 ‰ cf. 60-95 ‰), values of $\Delta(^{17}O)$ for snowpack NO_3^- are somewhat higher than those reported for atmospheric sources (aerosols, fog and precipitation) in a semiarid region of California (26 ±3 ‰; Michalski *et al*, 2004). Michalski et al. (2003) showed in a study of seasonal isotopic composition that $\Delta(^{17}O)$ values were consistently higher in winter months. The high values of $\Delta(^{17}O)$ found here are comparable to the few existing Arctic studies and indeed such high

15 values are only found in Polar regions (Morin et al., 2009). Morin et al. (2007a) reported $\Delta(^{17}O)$ values of 29-35 ‰ at Alert, Canada and 26-36 ‰ at Barrow, Alaska, compared with the present study where the coastal mean value of 30.8 ‰ was significantly lower than both Kelly Ville (mean = 34.4 ‰) and the ice sheet (mean = 33.8 ‰). However, some of the ice sheet samples in the current study ranged up to 43 ‰, higher than any previously recorded in the Arctic and comparable to data from Savarino et al. (2006) in Antarctica.

20

The non-mass dependent fraction of oxygen associated with tropospheric ozone means that there is positive correlation between ozone concentration and $\Delta(^{17}O)$ (Morin et al., 2007b). In Arctic coastal zones, springtime ozone depletion events commonly occur due to reaction pathways involving marine derived halogen compounds and radicals, most importantly linked to bromine (Morin et al., 2007b). Morin et al. (2007b) established a significant positive correlation between $\Delta(^{17}O)$

25 and ozone concentration and it may be speculated that the lower $\Delta(^{17}O)$ values in coastal snowpack in our study could be linked to ODE's caused by marine influences; although bromide was not measured, the contribution of sea salts to coastal snowpack in our study is very significantly greater than inland, suggesting a much greater potential for the influence of ODEs on $\Delta(^{17}O)$.

30 In the current study $\delta(^{15}N)$ is similar to seasonal snowpack data (Heaton et al., 2004) and ice cores (Vega et al., 2015a) from Svalbard, but highly depleted (regional means from -5.7 to -11.3 ‰) compared with data from ice cores obtained on the Greenland ice sheet, where NO_3^- over the last 300 years declined from a pre-industrial value near +11 ‰ to values around -1 ‰ in the last decade (Hastings et al., 2009) and is closely correlated with fossil fuel emissions since 1750. While the

decrease in $\delta(^{15}N)$ commenced around 1850, rising NO_3^- mass fractions in snow from the pre-industrial value of 73 ng g^{-1} only became apparent later, from around 1890, reaching 133 ng g^{-1} post 1950. The isotopic composition of NO_3^- in ice cores reflects Northern Hemisphere pollutants.

5   Hence there is a very strong gradient of declining snowpack $\delta(^{15}N)$ from the central ice sheet, to the ice sheet margin and with the most depleted values at the coast. There is clearly a major difference in the $\delta(^{15}N)$ of continuously accumulating snow on the central ice sheet compared with seasonal snowpack in the zone from the ice sheet margin to the coast. Such a strong spatial gradient must reflect either:

    i.   differing isotopic composition of inputs, due to differing sources of snowpack NO_3^- and/or fractionation during
10   transport to the deposition site (cf. Morin et al., 2009; Vega et al., 2015b), or

    ii.   a gradient in post-depositional processing and fractionation of NO_3^- between the coastal, inland and ice sheet sites.

4.3.1 Sources of snowpack NO_3^-

The linkages between the $\delta(^{15}N)$ of NO_3^- preserved in ice cores and anthropogenic sources are poorly understood and debated
15   in the literature and similar questions arise in our study where coastal snowpack $\delta(^{15}N)$ is much more depleted than values reported for many emission sources. Fibiger and Hastings (2016) reviewed the published ranges of $\delta(^{15}N)$ of NO_x and found that coal-fired power plant emissions were generally highly positive, while only soil emissions and automobile emissions included values of less than -10 ‰. Their own data on experimental biomass burning indicated values from -7 to +12 ‰ with the majority of materials giving positive values, although black spruce found in northern latitudes did give the most negative
20   values in their study. In a study of vehicle emissions which reported a wide range in $\delta(^{15}N)$ of NO_x from -19.1 to 9.8 ‰, it was found that emissions from diesel powered vehicles were the lowest (Walters et al., 2015a). In our coastal sites, it is possible that NO_x sources from diesel vehicles and shipping may contribute to snowpack NO_3^-, but while our coastal sites showed the lowest $\delta(^{15}N)$ values, other studies have found shipping emissions to be enriched in ^{15}N (Beyn et al., 2015). At the coast, the most enriched snowpack is found at AT5 closest to Sisimiut where there is a town with road vehicles, a port
25   and an airport, while at Kelly Ville the most enriched snowpack was found at SS02, closest to the harbour and Kangerlussuaq (Fig. 1; Supplementary Information Figure S.I.2). Hence while the influence of local sources cannot be ruled out, comparison of differences between catchments within regions does not support proximity to local sources as an explanation of the regional gradient in $\delta(^{15}N)$. An alternative hypothesis would be differences in source areas for long-range transported pollutants.

30

Heaton et al. (2004) speculate that preferential deposition of enriched NO_3^- leads to increasingly depleted NO_3^- with distance from source, while the later study of Vega et al. (2015b) supported the presence of such a process in air masses travelling long distances over the Arctic. In the present study, it is possible that this process could account for the very low $\delta(^{15}N)$

found especially in coastal snowpack, but is unlikely to account for the regional gradient observed. Given the relatively small distances involved (of the order of 100km from the ice sheet margin to the coast) relative to transport distances from possible N sources (assumed to be industrial regions in Europe, Siberia or North America), the large difference in snowpack $\delta(^{15}N)$ (regional differences >5 ‰) seems unlikely to be caused exclusively by this process. Burkhart et al. (2006) speculate that

5   the patterns of recent declining trends in ice-core NO_3^- since the 1990s suggest that Greenland snow may be recording European and North American NO_x and the distance of these sources from the study region are much greater than the within-region distances showing the gradient in isotopic composition.

Another possibility is that there could be a greater proportional contribution of dry deposition at the low precipitation inland

10   sites, relative to the coastal sites. Studies of daily variations in surface snow chemistry and isotopic composition at a coastal site in Svalbard indicated that increasing NO_3^- concentrations occurred between precipitation events, due to dry deposition inputs (Björkman et al., 2014). Since gas phase aerosol NO_3^- may be enriched in ^{15}N compared to wet deposited NO_3^-, such a mechanism could contribute to both the spatial patterns in NO_3^- concentrations and isotopic differences observed in our study. While the Svalbard study of Björkman et al. (2014) considered coastal snowpack and concluded that dry deposition

15   processes were likely to be more important than postdepositional processing, our study regions cover a strong climatic gradient with a much greater potential role for sublimation and photolytic effects on snowpack NO_3^- in inland sites.

4.3.2 Postdepositional processing

Higher levels of volatilisation of NO_3^- at the inland sites with greater sublimation and lower precipitation (cf. 250 mm SWE

20   at Summit; Dibb & Fahnestock, 2004) may lead to enrichment of snowpack ^{15}N compared with the coastal sites. Bosson et al. (2013) recorded sublimation rates at Two-Boat lake (our ice sheet site SS903) of 2.75 mm d^{-1} in April 2013. While these rates occurred during very favourable conditions for sublimation and are regarded as upper range values by the authors, they are two orders of magnitude greater than those recorded in the Svalbard study of Björkman et al. (2014) (0.042 mm d^{-1}) which ruled out postdepositional processing as a major determinant of snowpack NO_3^- concentrations and isotopic

25   composition. Heaton et al. (2004) and Morin et al. (2008) suggested that post-depositional processing of snowpack NO_3^- would lead to isotopic enrichment, so while these processes cannot account for the low coastal values, they could account for the higher inland values if it is assumed that fresh snow in all regions started from a similar value. A fresh snow sample collected at Kelly Ville did indeed show a much lower $\delta(^{15}N)$ of -11.8 ‰ (Table 5) compared with total snowpack in the region, but ad hoc rainfall samples at different times of year showed a variable $\delta(^{15}N)$. Since snow photochemistry is a major

30   driver of NO_3^- re-emissions, the effects of post-depositional processing should be maximal in spring when UV exposure is highest and there is still snowpack present (Morin et al., 2008).

The observed spatial isotopic gradient could potentially be the result of two opposing processes which could act to produce the same gradient; higher melting losses at the coast and higher sublimation losses inland. At the coast, higher temperatures may result in greater melting and preferential elution of the heavier isotope, leaving a more depleted snowpack. Inland, lower temperatures reduce melting effects but lower cloud cover and precipitation along with a much smaller snowpack

5   cause greater relative sublimation losses, leading to isotopic enrichment of the remaining snowpack. Such a process could explain the much more depleted $\delta(^{15}N)$ of -11.8 ‰ in fresh snow at Kelly Ville compared with a mean of -5.7 ‰ in total accumulated snowpack sampled at the same time of year but representing the net effect of postdepositional processing on the snowpack remaining at the end of the season.

10   While the relative importance of these processes cannot be determined conclusively from the current study, there are additional clues when comparing the terrestrial snowpack with the lake ice snowpack. At the coast and Kelly Ville, NO_3^- concentrations are significantly higher in lake ice snowpack than in terrestrial snowpack (Fig. 3) and it may be speculated that this could be due to meltwater losses draining from catchment slopes (with elevated ionic concentrations due to preferential elution) accumulating on the frozen lake surface. However, $\delta(^{15}N)$ values are generally lower in lake ice

15   snowpack than in the terrestrial snowpack (Fig S.I. 1) while the opposite might be expected if the lake ice snowpack was receiving enriched meltwater from the catchment. Hence the most plausible mechanism which could decrease NO_3^- concentrations on catchment slopes while increasing $\delta(^{15}N)$ would be greater volatilisation or sublimation losses of NO_3^- to the atmosphere.

20   Geng et al. (2014) argue that the high $\delta(^{15}N)$ in ice core records from the Greenland ice sheet relative to direct measurements of atmospheric sources may indicate a major role for post-depositional enrichment through volatilisation/evaporation and photolysis on the ice sheet during summer. Our data would support this assertion if it is assumed that coastal snowpack more closely represents the source isotopic composition while increased post-depositional processing occurs moving inland. The scope for such post-depositional enrichment is likely to increase from the coast to the ice sheet as precipitation levels and

25   snowpack accumulation rates decrease. Periodic melting events indicated by ice layers in the coastal snowpack may facilitate the downward transport of the relatively depleted NO_3^-, further reducing the potential for post-depositional processing via volatilisation or photolysis. The least depleted (or most enriched) $\delta^{15}N$ values in our study are found in the Kelly Ville region which has the lowest precipitation.

Burkhart et al. (2004) observed that almost all NO_3^- found in surface snow at Summit was still present in firn snow pits one

30   year later, while acknowledging that postdepositional NO_3^- loss to the atmosphere may occur and can be offset by dry deposition of HNO_3. Concentrations of sulfate and NO_3^- in firn are strongly affected by snow accumulation rates and this is particularly important for accumulation of NO_3^- in snowpack since high NO_3^- re-emission losses have been recorded in low accumulation areas such as central Antarctica (Fischer et al., 1998a). Likewise, Dibb et al. (2007) found NO_3^- concentrations to be 9% higher in surface snow than in buried snow and concluded that postdepositional losses of NO_3^- may be as high as

25% within 1-2 years of deposition. They attributed postdeposition losses of volatile species on ice grain surfaces to decreases in surface area/volume ratios due to ice grain growth, or to photolysis, while non-volatiles may increase due to either dry deposition and/or loss of water mass by sublimation. Postdeposition processing is likely to play a more significant role in areas of higher temperatures and/or lower accumulation rates (Burkhart et al., 2004; Fischer et al., 1998a). For the

5   purpose of calculating net deposition rates to catchments and receiving lake basins, the net effects (photochemical losses and gains) on NO_3^- through postdepositional processing throughout the snow accumulation season should be accounted for by sampling at the end of the season.

4.3.3 Seasonal variations in $\delta(^{15}N)$ of deposited NO_3^-

10   Ice core data show seasonal variation in the recent isotopic signature, with summer values higher than winter, which was not apparent in pre-industrial ice (Hastings et al., 2004, 2009). The depletion of $\delta(^{15}N)$ has been strongest in winter. Since our study records only winter deposition inputs, it is likely that we are capturing the most depleted component of annual inputs leading to lower values than annually resolved records on the ice sheet, where snowpack continuously accumulates through the year (Dibb & Fahnestock, 2004). Morin et al. (2008) recorded strong seasonal variations in atmospheric $\delta(^{15}N)$ on the ice

15   sheet, with lowest values of -15 ‰ in winter through to March, and asserted that emissions of reactive N from snowpack during spring resulted in an increase of $\delta(^{15}N)$ in remaining NO_3^-. Hastings et al. (2004) found a strong seasonal variation in the $\delta(^{15}N)$ of fresh snow, with minimal mean values in winter of -10 ‰, and even recorded diurnal variations in deposited snow, with more enriched snow samples collected during the day and more depleted at night. They attributed this diurnal signal to redeposition of NOx emitted from the snowpack during the day, either through direct contact with the snow surface

20   or during fog events. These patterns are consistent with the spatial gradient in the current study, where the most depleted snowpack $\delta(^{15}N)$ was found at the coast, where higher precipitation (and accumulation) and greater incidence of cloud cover and fog would reduce the potential for re-emission of depleted N from the snowpack. The few rainfall samples analysed during late summer for all regions show a higher $\delta(^{15}N)$ than the snowpack samples, while the sole rain sample analysed from spring (May 2011) at the ice sheet margin had the lowest value in rain, but still not as low as snowpack. Such

25   postdepositional processing in combination with seasonal changes found on the ice sheet, and hinted at in our rainfall data, could explain the major differences between our coastal snowpack samples (reflecting minimal winter deposition) and those recorded at Summit (reflecting year round accumulation including much more enriched summer deposition).

5. Conclusions

30   There is a strong gradient in snowpack accumulation and SWE from inland to the coast, reflecting the annual precipitation which is twice as high at the coast than inland. Late season snowpack in SW Greenland shows a strong chemical gradient

from the ice sheet margin to the coast. For inland snowpack, chemistry is comparable to remote locations such as Summit on the central ice sheet as well as other Arctic locations remote from industrial sources. At the coast, sea salt ions dominate the accumulated snowpack, but are much less important in fresh snow. While NO_3^- is the dominant ion at Summit (Dibb et al., 2007) its concentration declines from inland regions to the coast. However the reverse is true for NH_4^+ and nss-SO_4^{2-} with

5   significantly higher concentrations in coastal snowpack than inland. Marine-derived aerosols of ammonium sulfate may be a possible source of these ions in coastal snowpack.

A lack of summer rainfall chemistry data prevents accurate estimation of annual deposition fluxes, but net deposition inputs to catchments may be approximated by assuming (on the basis of a small number of *ad hoc* rainfall samples) that snowpack

10   chemistry is representative of annual mean precipitation, since snow represents around half of annual precipitation. On this assumption there is a strong deposition gradient from inland to the coast, which is much more pronounced for NH_4^+ and nss-SO_4^{2-} than for NO_3^-. While NO_3^- deposition ranges from 0.08-0.13 kg ha^{-1} a^{-1}, comparable to fluxes at Summit (Burkhart et al., 2004), total inorganic N deposition fluxes are almost 2-3 times higher at the coast (0.37 kg ha^{-1} a^{-1}) than inland, primarily due to NH_4^+. These values are within the range of other studies from remote Arctic locations. In equivalence terms, NO_3^-

15   deposition is very similar to nss-SO_4^{2-} at inland locations, but less than half at the coast. However NH_4^+ is more comparable to nss-SO_4^{2-} at the coast where TIN is about 23% higher than nss-SO_4^{2-}, compared with around double at inland locations.

While chemistry and deposition show similarities to ice sheet snowpack, stable isotope data show major differences. There is a gradient of declining $\delta^{15}N$ from the inland areas to the coast, but samples are all highly depleted compared with samples

20   from Summit, with regional means from -5.7 to -11.3‰ compared with only -1‰ in recent Summit ice core samples. While differences in emissions sources are possible, post-depositional processing of snowpack NO_3^- seems the most plausible mechanism driving this very strong gradient in N fractionation. The processes which best explain both the spatial gradient and also the observed differences between snowpack on catchment slopes and lake ice snowpack are sublimation and volatilization. These processes can act to reduce NO_3^- concentrations while simultaneously increasing the remaining

25   snowpack $\delta(^{15}N)$. Hence lower NO_3^- concentrations in coastal snowpack are due to the diluting effect of much higher precipitation, but lower concentrations on catchment slopes within each region compared with lake ice snowpack are due to enhanced losses to the atmosphere. Overall, the isotopic composition of coastal snowpack reflects the low $\delta(^{15}N)$ of winter deposition observed in other studies at Summit and Svalbard, but the current study demonstrates for the first time the spatial gradients in snowpack isotopes resulting from the climatic gradient from the coast to the ice sheet.

30

Future changes in climate are likely to affect the gradients in snowpack chemistry, stable isotopes and deposition observed in the current study, given the importance of precipitation and other climatic factors in driving spatial differences. In 2012 the coastal town of Sisimiut recorded its highest annual precipitation since records began (1004mm) and this AWS station shows the strongest increasing precipitation trend across the Greenland network of +48.5 mm a^{-2} from 2001-2012 (Mernild et al.,

2015). Over the same period, Kangerlussuaq and the closest ice sheet sites showed decreasing trends in precipitation. It has also been speculated that climate change will affect the relative importance of source types and regions for deposition in the Arctic. While some of these sources are closely linked to industrial activity in the Arctic regions of Europe and the Russian Federation, emissions from forest fires and shipping activity could both increase with climatic warming in the Arctic polar

5   region (Hole et al.,2006b).

Author contributions

C. J. Curtis, N.J. Anderson, G. Simpson and J. Kaiser designed the study. Curtis, Anderson, Simpson, Jones and Whiteford carried out fieldwork and sample preparation. Kaiser and Marca carried out laboratory analyses. All authors contributed to

10   writing and interpretation of the data.

Competing interests

The authors declare that they have no conflict of interest.

15   **Data availability**

All underlying site location, chemistry and isotope data are publicly available via the following link: (DOI to follow)

References

AMAP: AMAP Assessment 2006: Acidifying Pollutants, Arctic Haze and Acidification in the Arctic, Arctic Monitoring and Assessment Programme (AMAP), Oslo, Norway, xii+112pp, 2006.

Bates, D., Maechler, M., Bolker, B. and Walker, S.: Fitting Linear Mixed-Effects Models Using lme4. Journal of Statistical Software, 67(1), 1-48, doi:10.18637/jss.v067.i01, 2015.

Bergström, A. K. and Jansson, M.: Atmospheric nitrogen deposition has caused nitrogen enrichment and eutrophication of lakes in the northern hemisphere, Global Change Biology, 12, 635-643, 2006.

Bindler, R., Renberg, I., Appleby, P. G., Anderson, N. J. and Rose, N. L.: Mercury accumulation rates and spatial patterns in lake sediments from West Greenland: a coast to ice margin transect, Environ. Sci. Technol., 35, 1736-1741, 2001a.

Bindler, R., Renberg, I., Anderson, N. J., Appleby, P. G., Emteryd, O. and Boyle, J.: Pb isotope ratios of lake sediments in West Greenland: inferences on pollution sources, Atmospheric Environment, 35, 4675-4685, 2001b.

Björkman, M. P., Vega, C. P., Kühnel, R., Spataro, F., Ianniello, A., Esposito, G., Kaiser, J., Marca, A., Hodson, A., Isaksson, E. and Roberts, T. J.: Nitrate postdeposition processes in Svalbard surface snow, *J. Geophys. Res.,* 119, 12953, 10.1002/2013JD021234, 2014.

Bosson, E., Lindborg, T., Berglund, S., Gustafsson, L. -G., Selroos, J. -O., Laudon, H., Claesson, L. L. and Destouni, G.: Water balance and its intra-annual variability in a permafrost catchment: hydrological interactions between catchment, lake and talik, Hydrol. Earth. Syst. Sci. Discuss.*,* 10, 9271-9308, 2013.

Burkhart, J. F., Hutterli, M. A., Bales, R. C. and McConnell, J. R.: Seasonal accumulation, timing and preservation of nitrate in firn at Summit, Greenland, Journal of Geophysical Research-Atmospheres, 109, D19302, doi10.1029/2004JD004658, 2004.

Burkhart, J. F., Bales, R. C., McConnell, J. R. and Hutterli, M. A.: Influence of North Atlantic Oscillation on anthropogenic transport recorded in northwest Greenland ice cores, Journal of Geophysical Research-Atmospheres, 111, D22309, doi: 10.1029/2005JD006771, 2006.

Casciotti, K. L., Sigman, D. M., Hastings, M. G., Böhlke, J. K., Hilkert, A.: Measurement of the oxygen isotope composition of nitrate in seawater and freshwater using the denitrifier method, Analytical Chemistry, 74, 4905-4912, 2002.

Clow, D. W., Ingersoll, G. P., Mast, A., Turk, J. T. and Campbell, D. H.: Comparison of snowpack and winter wet-deposition chemistry in the Rocky Mountains, USA: implications for winter dry deposition, Atmospheric Environment, 36, 2337-2348, 2002.

de Caritat, P., Hall, G., Gìslason, S., Belsey, W., Braun, M., Goloubeva, N. I., Olsen, H. K., Scheie, J. O. and Vaive, J. E.: Chemical composition of arctic snow: concentration levels and regional distribution of major elements, Science of the Total Environment, 336, 183-199, 2005.

Davies, T. D., Vincent, C. E. and Brimblecombe, P.: Preferential elution of strong acids from a Norwegian ice cap, Nature, 300, 161-163, 1982.

Dibb, J. E. and Fahnestock, M.: Snow accumulation, surface height change, and firn densification at Summit, Greenland, J. Geophys. Res,. 109, D24113, doi:10.1029/2003JD004300, 2004.

Dibb, J. E., Whitlow, S. I. and Arsenault, M.: Seasonal variations in the soluble ion content of snow at Summit, Greenland: constraints from three years of daily surface snow samples, Atmospheric Environment, 41, 5007-5019, 2007.

5   Fibiger, D. L., Dibb, J. E., Chen, D., Thomas, J. L., Burkhart, J. F., Huey, L. G. and Hastings, M.G.: Analysis of nitrate in the snow and atmosphere at Summit, Greenland: chemistry and transport, *J. Geophys. Res. Atmos.*, 121, doi: 10.1002/2015JD024187, 2016.

Fischer, H., Wagenbach, P. and Kipfstuhl, J.: Sulfate and nitrate firn concentrations on the Greenland ice sheet. 1. Large-scale geographical deposition changes, Journal of Geophysical Research-Atmospheres, 103, 21927-21934, 1998a.

10   Fischer, H. Wagenbach, P. and Kipfstuhl, J.: Sulfate and nitrate firn concentrations on the Greenland ice sheet. 2. Temporal and anthropogenic deposition changes, Journal of Geophysical Research-Atmospheres, 103, 21935-21942, 1998b.

Fisher, J. A., Jacob, D. J., Wang, Q., Bahreini, R., Carouge, C. C., Cubison, M. J., Dibb, J. E., Diehl, T., Jimenez, J. L., Leibensperger, E.M., Lu, Z., Meinders, M. B. J., Pye, H. T., Quinn, P. K., Sharma, S., Streets, D. G., Van Donkelaar, A. and Yantosca, R. M.: Sources, distribution, and acidity of sulfate-ammonium aerosol in the Arctic in winter-spring,
15   Atmospheric Environment, 45 (39), 7301-7318 2011.

Geng, L., Alexander, B., Cole-Dai, J., Steig, E. J., Savarino, J., Sofen, E. D. and Schauer, A. J.: Nitrogen isotopes in ice core nitrate linked to anthropogenic acidity change, PNAS, 111, 5808-5812, 2014.

Hanna, E., Mernild, S. H., Cappelen, J. and Steffen, K.: Recent warming in Greenland in a long-term instrumental (1881-2012) climatic context: I. Evaluation of surface air temperature records, Environ. Res. Lett., 7, 045404, 2012.

20   Hastings, M. G., Steig, E. J. and Sigman, D. M.: Seasonal variations in N and O isotopes of nitrate in snow at Summit, Greenland: implications for the study of nitrate in snow and ice cores, J. Geophys. Res., 109, D20306, doi: 10.1029/2004JD004991, 2004.

Hastings M. G., Jarvis, J. C. and Steig, E. J.: Anthropogenic impacts on nitrogen isotopes of ice core nitrate, Science, 324, 1288, 2009.

25   Heaton, T. H. E., Wynn, P. and Tye, A. M.: Low ^{15}N/^{14}N ratios for nitrate in snow in the High Arctic (79°N), Atmospheric Environment, 38, 5611-5621, 2004.

Hole, L. R., Christensen, J., Ginzburg, V. A., Makarov, V., Pershina, N. A., Polischuk, A. I., Ruoho-Airola, T., Svistov, P. P. and Vasilenko, V. N.: Chapter 3: Concentrations and deposition of acidifying pollutants, in: AMAP Assessment 2006: Acidifying Pollutants, Arctic Haze and Acidification in the Arctic, Arctic Monitoring and Assessment Programme
30   (AMAP), Oslo, Norway, 11-30, 2006a.

Hole, L. R., Christensen, J., Forsius, M., Nyman, M., Stohl, A. and Wilson, S.: Chapter 2: Sources of acidifying pollutants and arctic haze precursors, in: AMAP Assessment 2006: Acidifying Pollutants, Arctic Haze and Acidification in the Arctic, Arctic Monitoring and Assessment Programme (AMAP), Oslo, Norway, 2-9, 2006b.

Hole, L. R., Christensen, J. H., Ruoho-Airola, T., Tørseth, K., Ginzburg, V. and Glowacki, P.: Past and future trends in
35   concentrations of sulfur and nitrogen compounds in the Arctic, Atmospheric Environment, 43, 928-939, 2009.

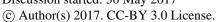Holtgrieve, G. W., Schindler, D. E., Hobbs, W. O., Leavitt, P. R., Ward, E. W., Bunting, L., Chen, G., Finney, B. P., Gregory-Eaves, I., Holmgren, S., Lisac, M. J., Lisi, P. J., Nydick, K., Rogers, L. A., Saros, J. E., Selbie, D. T., Shapley, M. D., Walsh, P. B. and Wolfe, A. P.: A coherent signature of anthropogenic nitrogen deposition to remote watersheds of the northern hemisphere, Science, 334, 1545-1548, 2011.Hothorn, T., Bretz, F. and Westfall, P.: Simultaneous Inference
5   in General Parametric Models, Biometrical Journal, 50(3), 346—363, 2008.

Ingersoll, G. P., Mast, A., Campbell, D. H., Clow, D. W., Nanus, L. and Turk, J.T.: Trends in snowpack chemistry and comparison to National Atmospheric Deposition Program results for the Rocky Mountains, USA, 1993-2004, Atmospheric Environment, 42, 6098-6113 2008.

Ingersoll, G. P., Campbell, D., Mast, M. A., Clow, D. W., Nanus, L. and Frakes, B.: Snowpack chemistry monitoring
10   protocol for the Rocky Mountain Network; narrative and standards operating procedures, USGS Administrative Report, U.S. Geological Survey, Reston, Virginia, USA, 47pp, 2009.

Jaffe, D. A. and Zukowski, M. D.: Nitrate deposition to the Alaskan snowpack, Atmos. Env., 27A, 2935-2941, 1993.

Johansson, E., Berglund, S., Lindborg, T., Petrone, J., van As, D., Gustafsson, L. -G., Näslund, J. -O. and Laudon, H.: Hydrological and meterorological investigations in a periglacial lake catchment near Kangerlussuaq, west Greenland –
15   presentation of a new multi-parameter data set, Earth. Syst. Sci. Data, 7, 93-108, 2015.

Kaiser, J., Hastings, M. G., Houlton, B. Z., Rockmann, T. and Sigman, D. M.: Triple oxygen isotope analysis of nitrate using the denitrifier method and thermal decomposition of N_2O, Analytical Chemistry, 79, 599-607, 2007.

Mayewski, P. A., Lyons, W. B., Spencer, M. J., Twickler, M. S., Buck, C. F. and Whitlow, S.: An ice core record of atmospheric response to anthropogenic sulfate and nitrate, Nature, 346, 554-556, 1990.

20   Mernild, S. H., Hanna, E., McConnell, J. R., Sigl, M., Beckerman, A. P., Yde, J. C., Cappelen, J., Malmros, J. K. and Steffen, K.: Greenland precipitation trends in a long-term instrumental climate context (1890-2012): evaluation of coastal and ice core records, Int. J. Climatology, 35, 303-320, 2015.

Michalski, G., Scott, Z., Kabiling, M. and Thiemens, M. H.: First measurements and modeling of $\Delta^{17}O$ in atmospheric nitrate, Geophys. Res. Lett., 30(16), 1870, doi:1810.1129/2003GL017015, 2003.

25   Michalski, G., Meixner, T., Fenn, M., Hernandez, L., Sirulnik, A., Allen, E. and Thiemens, M.: Tracing atmospheric nitrate deposition in a complex semiarid ecosystem using $\Delta^{17}O$, Environmental Science and Technology, 38, 2175-2181, 2004.

Morin, S., Savarino, J., Bekki, S., Cavender, A., Shepson, P. B. and Bottenheim, J. W.: Major influence of BrO on the NO_x and nitrate budgets in the Arctic spring, inferred from $\Delta^{17}O(NO_3^-)$ measurements during ozone depletion events, Environmental Chemistry, 4, 238, 10.1071/en07003, 2007a.

30   Morin, S., Savarino, J., Bekki, S., Gong, S. and Bottenheim, J. W.: Signature of Arctic surface ozone depletion events in the isotope anomaly ($\Delta^{17}O$) of atmospheric nitrate, Atmos. Chem. Phys., 7, 1451, 2007b.

Morin, S., Savarino, J., Frey, M. M., Yan, N., Bekki, S., Bottenheim, J. W. and Martins, J. M. F.: Tracing the origin and fate of NOx in the Arctic atmosphere using stable isotopes in nitrate, Science, 322, 730-732, 2008.
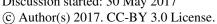
Morin, S., Savarino, J., Frey, M. M., Domine, F., Jacobi, H.W., Kaleschke, L., Martins, J. M. F.: Comprehensive isotopic composition of atmospheric nitrate in the Atlantic Ocean boundary layer from 65ºS to 79ºN, J. Geophys. Res., 114, D05303, 2009.

Paulot, F., Jacob, D. J., Johnson, M. T., Bells, T. G., Baker, A. R., Keene, W. C., Lima, I. D., Doney, S. C. and Stock, C. A.: Global oceanic emission of ammonia: constraints from seawater and atmospheric observations, Atmos. Chem. Phys., 9, 8883–8888, 2015.

Pedersen, S. H., Liston, G.E., Tamstorf, M.P., Westergaard-Nielsen, A., Schmidt, N.M. (2015) Quantifying episodic snowmelt events in Arctic ecosystems. *Ecosystems*, 18: 839-856.

R Core Team: R: A language and environment for statistical computing, R Foundation for Statistical Computing, Vienna, Austria, URL https://www.R-project.org/, 2016.

Smol, J. P., Wolfe, A. P., Birks, H. J. B., Douglas, M. S. V., Jones, V. J., Korhola, A., Pienitz, R., Rühland, K., Sorvari, S., Antoniades, D., Brooks, S. J., Fallu, M. -A., Hughes, M., Keatley, B. E., Laing, T. E., Michelutti, N., Nazarova, L., Nyman, M., Paterson, A. M., Perren, B., Quinlan, R., Rautio, M., Saulnier-Talbot, E., Siitonen, S., Solovieva, N. and Weckström, J. Climate-drive regime shifts in the biological communities of arctic lakes, Proc. Nat. Acad. Sci., 102, 4397-4402, 2005.

Sturm, M., Taras, B., Liston, G. E., Derksen, C., Jonas, T. and Lea, J.: Estimating snow water equivalent using snow depth data and climate classes, Journal of Hydrometeorology, 11, 1380-1394, 2010.

Turk, J. T., Taylor, H. E., Ingersoll, G. P., Tonnessen, K. A., Clow, D. W., Mast, M. A., Campbell, D. H. and Melack, J. M.: Major-ion chemistry of the Rocky Mountain snowpack, USA, Atmospheric Environment, 35, 3957-3966, 2001.

Tye, A. M., Heaton, T. H. E.: Chemical and isotopic characteristics of weathering and nitrogen release in non-glacial drainage waters on Arctic tundra, Geochimica et Cosmochimica Acta, 71, 4188-4205, 2007.

Vega, C. P., Pohjola, V. A., Samyn, D., Pettersson, R., Isaksson, E., Björkman, M. P., Martma, T., Marca, A. and Kaiser, J.: First ice core records of NO3− stable isotopes from Lomonosovfonna, Svalbard, J. Geophys. Res., 120, 313, 10.1002/2013JD020930, 2015a.

Vega, C. P., Björkman, M. P., Pohjola, V. A., Isaksson, E., Pettersson, R., Martma, T., Marca, A. and Kaiser, J.: Nitrate stable isotopes in snow and ice samples from four Svalbard sites, Polar Research, 34, 23246, 10.3402/polar.v34.23246, 2015b.

Vet, R., Artz, R. S., Carou, S., Shaw, M., Ro, C. -U., Aas, W., Baker, A., Bowersox, V. C., Dentener, F., Galy-Lacaux, C., Hou, A., Pienaar, J. J., Gillett, R., Forti, M. C., Gromov, S., Hara, H., Khodzher, T., Mahowald, N. M., Nickovic, S., Rao, P. S. P. and Reid, N. W.: A global assessment of precipitation chemistry and deposition of sulfur, nitrogen, sea salt, base cations, organic acids, acidity and pH, and phosphorus, Atmospheric Environment, 93, 3-100, 2014.

Williams, M. W., Seibold, C. and Chowanski, K.: Storage and release of solutes from a subalpine seasonal snowpack: soil and stream water response, Niwot Ridge, Colorado, Biogeochemistry, 95, 77-94, 2009.

Yang, D., Ishida, S., Goodison, B. E. and Gunther, T.: Bias correction of daily precipitation measurements for Greenland, J. Geophys. Res., 104, D6, 6171-6181.

Figure 1: Location of sampling regions and catchments within west Greenland

Figure 2: a) Typical sublimating snowpack close to the ice sheet and lake ice snowcover on lake SS903 (24th March 2011), b) contrasting with deep snow profile on lower catchment slope of coastal site AT7 two days later (26th March 2011)

Figure 3: Comparison of regional snowpack ion concentrations (aggregated data – n=24 per region; all units in μmol L^{-1}). Boxes represents 25th and 75th percentiles, horizontal line = median, whiskers show data extent, points indicate outliers (1.5-3 IQRs outside box)

5

Figure 4: Comparison of lake ice (red) and terrestrial (blue) snowpack concentrations (μmol L^{-1}) for selected ions. See Fig. 3 caption for explanation of boxplots.

Figure 5: Comparison of regional aggregated (n=24 per region) snowpack stable isotopes. See Fig.3 caption for explanation of boxplots.

Table 1: Sampling catchment details (based on centroid of lakes)

Region	Site	Latitude (° N)	Longitude (° W)	Altitude (m)	Lake area (ha)	Catchment area (ha)
Ice Sheet	SS906	67.120	50.256	415	9.3	50.6
Ice Sheet	SS903	67.130	50.172	315	38.0	117
Ice Sheet	SS904	67.157	50.278	405	12.4	42.5
Kelly Ville	SS02	66.996	50.964	160	36.8	217
Kelly Ville	SS08	67.013	51.075	163	14.6	278
Kelly Ville	SS1333	67.001	51.146	308	13.8	57.5
Coast	AT1	66.967	53.404	445	8.0	49.7
Coast	AT7	66.972	53.585	324	6.5	203
Coast	AT5	66.961	53.679	117	7.5	443

5   **Table 2: Snow depth measurements and snow water equivalents (SWE) by catchment and region**

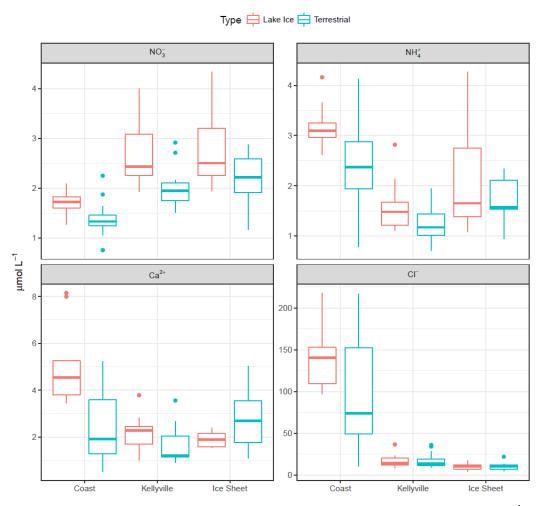| Site / Region	Area (ha)	Altitude (m) Lake/Min.	Max.	n	Snow depth (cm) Range	Mean	SD	n	SWE (mm) Mean	SD	Corr. SWE (mm) *
SS906	50.6	415	463	64	1-55	20.1	13.9	48	37.9	35.9	34.5
SS903	117	315	476	155	0-74	20.0	13.9	58	43.9	45.8	38.6
SS904	42.5	405	487	104	0-103	16.1	17.5	26	49.9	54.9	35.1
Ice Sheet		**315**	**487**	**323**	**0-103**	**18.8**	**15.2**	**132**	**42.9**	**44.4**	**35.7**
SS02	217	160	372	123	0-65	20.5	12.0	65	39.1	27.7	35.3
SS08	278	163	279	120	2-50	23.8	10.7	49	49.6	33.9	48.8
SS1333	57.5	308	355	94	1-100	24.4	15.3	39	53.3	41.7	48.6
Kelly Ville		**160**	**372**	**337**	**0-100**	**22.8**	**12.7**	**153**	**46.1**	**34.0**	**43.6**
AT1	49.7	445	558	102	0-240	73.5	52.8	48	187.9	119.3	196.1
AT7	203	324	441	111	1-260	49.7	43.6	48	149.7	93.6	161.3
AT5	443	117	197	112	5-250	66.9	47.0	45	135.6	89.9	181.8
Coast		**117**	**551**	**325**	**0-260**	**63.1**	**48.7**	**141**	**158.0**	**103.5**	**180.8**

*Mean SWE corrected for larger number of snow depth-only measurements

Table 3a: Catchment terrestrial snowpack sampling details (n=5 per catchment)

Region	Site	Date	Altitude (m)	Depth (cm)	Air temp (°C)	Snow temp (°C)
Ice Sheet	SS906	23/03/2011	430-440	24-34	-18 to -22	-14 to -27
Ice Sheet	SS903	24/03/2011	333-371	27-74	-10 to -18	-6 to -20
Ice Sheet	SS904	30/03/2011	421-450	25-103	-6 to -11.5	-4 to -8.5
Kelly Ville	SS02	22/03/2011	192-260	23-65	-16 to -25	-13 to -31
Kelly Ville	SS08	31/03/2011	198-211	40-48	-8 to -11	-8.5 to -13.5
Kelly Ville	SS1333	01/04/2011	317-349	27-49	-9 to -15	-7 to -11
Coast	AT1	27/03/2011	478-558	28-240	0 to 2	-2.5 to -9
Coast	AT7	26/03/2011	346-362	31-238	4 to 6	-0.5 to -9
Coast	AT5	28/03/2011	132-143	74-141	-1 to 0.5	-1.5 to -7

Table 3b: Lake ice snowpack sampling details (n=3 per lake)

Region	Site	Date	Altitude (m)	Depth (cm)	Air temp (°C)	Snow temp (°C)
Ice Sheet	SS906	23/03/2011	421-430	12-23	-18	-10 to -18
Ice Sheet	SS903	24/03/2011	333-340	8-13	-12 to -18	-11 to -15
Ice Sheet	SS904	30/03/2011	414-430	5-10	-11 to -12	-5 to -8
Kelly Ville	SS02	02/04/2011	169-180	15-23	-9 to -12	-6 to -9
Kelly Ville	SS08	31/03/2011	166-178	20-30	-8 to -11	-6 to -10.5
Kelly Ville	SS1333	01/04/2011	311-323	20-25	-12 to -15	-7 to -15
Coast	AT1	27/03/2011	456-463	35-44	4 to 5	-0.5 to -2
Coast	AT7	26/03/2011	336-344	19-32	1 to 5	-0.5 to -5
Coast	AT5	28/03/2011	128-133	25-60	0 to 0.5	-1 to -3

5

Table 4: Comparison of aggregated snowpack chemistry (n=24 per region), derived non-marine concentrations of major ions (all in µmol L^{-1}) and stable isotopes (per mille). See text for details of post-hoc pairwise comparisons. Coast = CO, Kelly Ville = KV, ice sheet = IS.

Region:	Coast (CO)		Kelly Ville (KV)		Ice Sheet (IS)		Post hoc sig. differences		
Analyte	Mean	SD	Mean	SD	Mean	SD	CO-KV	CO-IS	KV-IS
Nutrients									
NO$_2^-$	**0.0**	0.0	**0.0**	0.0	**0.1**	0.4			
NH$_4^+$	**2.7**	0.9	**1.4**	0.5	**1.9**	0.8	0.0017		
NO$_3^-$	**1.5**	0.4	**2.3**	0.6	**2.4**	0.6	<0.0001	<0.0001	
PO$_4^{3-}$	**0.0**	0.0	**0.1**	0.1	**0.1**	0.2	<1e-05	<1e-05	
Base cations									
Ca^{2+}	**3.5**	2.0	**1.8**	0.8	**2.5**	1.0	<0.001		
Mg^{2+}	**13.8**	7.4	**2.6**	1.2	**2.5**	1.1	<1e-08	<1e-08	
K$^+$	**2.8**	1.4	**0.8**	0.3	**0.8**	0.5	<1e-05	<1e-05	
Na$^+$	**86.9**	48.5	**12.2**	6.0	**7.1**	3.1	<0.001	<0.001	
Anions									
Cl$^-$	**114.4**	61.0	**17.2**	8.6	**10.3**	4.3	<0.0001	<0.0001	
SO$_4^{2-}$	**7.7**	4.2	**2.4**	2.6	**1.8**	0.6	<0.0001	<0.0001	
Non-sea salt									
nss-Ca^{2+}	**1.4**	1.4	**1.6**	0.7	**2.3**	1.0	<1e-08	<1e-08	<1e-08
nss-Mg^{2+}	**2.4**	1.8	**0.9**	0.5	**1.5**	0.9	<0.001		0.014
nss-K$^+$	**0.7**	0.4	**0.5**	0.3	**0.6**	0.4			
nss-Na$^+$	**-11.5**	4.5	**-2.5**	1.3	**-1.8**	1.1			
nss-SO$_4^{2-}$	**1.8**	1.8	**1.0**	0.4	**1.2**	0.5	0.0011	0.0358	
Isotopes									
δ(^{15}N)	**-11.3**	1.3	**-5.7**	2.3	**-7.5**	2.2	<0.0001	0.001	
δ(^{18}O)	**81.7**	2.8	**81.9**	3.5	**83.3**	2.9			
Δ(^{17}O)	**30.8**	3.7	**34.4**	2.8	**33.8**	3.3	<0.001	0.0052	

5

Table 5: Comparison of *ad hoc* rain and fresh snow samples with mean snowpack data (from Table 4 - italics) (concentrations in μmol L^{-1}; isotopes in ‰)

Location	Sample type	Sample dates	NH$_4^+$	NO$_3^-$	PO$_4^{3-}$	Ca^{2+}	K$^+$	Mg^{2+}	Na$^+$	Cl$^-$	SO$_4^{2-}$	δ(^{15}N)	δ(^{18}O)	Δ(^{17}O)
SS903	Rain	18/05/11-23/05/11	3.6	5.0	0.2	6.2	0.2	1.8	7.8	9.3	3.0	-10.0	81.9	30.3
SS906	Rain	05/09/12-06/09/12	2.6	1.7	0.2	9.0	2.6	2.8	13.8	18.3	2.0	-5.6	60.8	20.6
Ice Sheet	**Rain**	**Mean**	**3.1**	**3.4**	**0.2**	**7.6**	**1.4**	**2.3**	**10.8**	**13.8**	**2.5**	**-7.8**	**71.4**	**25.5**
Ice Sheet	*Snowpack*	*Mean*	*1.9*	*2.4*	*0.3*	*2.5*	*0.8*	*2.6*	*7.1*	*10.3*	*1.8*	*-7.5*	*83.3*	*33.8*
SS02	Rain	08/08/11-24/08/11	1.4	7.8	0.1	12.3	0.6	2.1	14.1	16.8	4.1	0.9	70.9	22.7
SS02	Rain	28/08/11-01/09/11	1.3	5.2	0.0	7.6	3.5	0.7	5.7	4.1	1.5	-0.9	76.4	23.1
SS02	Rain	01/09/11-07/09/11	0.3	1.8	0.1	6.2	0.3	0.8	4.2	3.8	1.4	-3.4	63.3	21.9
Kanger.	Rain	05/09/12-06/09/12	0.2	1.3	0.1	15.0	0.5	2.4	9.3	10.2	1.9	0.4	55.4	-
Kelly Ville	**Rain**	**Mean**	**0.8**	**4.0**	**0.1**	**10.3**	**1.2**	**1.5**	**8.3**	**8.7**	**2.2**	**-0.8**	**66.5**	**22.6**
SS1333	Snow Fresh	01/04/11	3.4	3.4	0.3	1.9	0.9	2.7	13.5	18.8	2.6	-11.8	84.2	31.4
Kelly Ville	*Snowpack*	*Mean*	*1.4*	*2.3*	*0.3*	*1.9*	*0.8*	*2.6*	*12.2*	*17.2*	*2.4*	*-5.7*	*81.9*	*34.4*
AT5	Snow Fresh	28/03/11	4.6	4.7	0.0	1.2	0.5	2.2	10.6	16.3	2.3	-10.2	83.6	31.2
Coast	*Snowpack*	*Mean*	*2.7*	*1.5*	*0.0*	*3.5*	*2.8*	*13.8*	*86.9*	*114.4*	*7.7*	*-11.3*	*81.7*	*30.8*

5

Table 6: Mean annual meteorological data and deposition estimates based on snowpack chemistry and mean precipitation (2001-12) for Sisimiut (coast), Kangerlussuaq and SS903 at the ice sheet margin (Bosson et al., 2013; Mernild et al., 2015). #Data from Whiteford et al. (2016) are 2011 mean values except Kangerlussuaq (Kelly Ville) wind speed, which is from 2010

Region	Pptn	Temp[#]	Wind speed[#]	N in NO$_3^-$	N in NH$_4^+$	TIN	S in nss-SO$_4^{2-}$	NO$_3^-$	NH$_4^+$	TIN	nss-SO$_4^{2-}$
	mm	°C	m s^{-1}	kg ha^{-1} a^{-1}				mol ha^{-1} a^{-1}			
Coast	631	-2.1	2.9	0.13	0.24	0.37	0.35	9	17	27	11
Kelly Ville	258	-5.6	3.6	0.08	0.05	0.13	0.08	6	4	10	3
Ice sheet	320	-5.0	4.0	0.11	0.09	0.19	0.13	8	6	14	4

10